A caged tris(2-pyridylmethyl)amine ligand equipped with a C triazole –H hydrogen bonding cavity

Gege Qiu, Donglin Diao, Leo Chaussy, Sabine Michaud-Chevallier, A. Jalila Simaan, Paola Nava, Alexandre Martinez, Cédric Colomban

A caged tris(2-pyridylmethyl)amine ligand equipped with a C$_{triazole}$-H hydrogen bonding cavity.

Gege Qiu,[‡a] Donglin Diao,[‡a] Leo Chaussy,[a] Sabine Michaud-Chevallier,[a] Paola Nava,[a] Alexandre Martinez*[a] and Cédric Colomban*[a]

A CAPPED BIOINSPIRED LIGAND BUILT FROM A TRIS(2-PYRIDYL-METHYL)AMINE (TPA) UNIT AND SURMOUNTED BY A TRIAZOLE-BASED INTRAMOLECULAR H-BONDING SECONDARY SPHERE, WAS PREPARED. THE RESULTING CAGE PROVIDES A WELL-DEFINED CAVITY COMBINING A HYDROPHOBIC NATURE WITH H-BONDING PROPERTIES. ITS COORDINATING PROPERTIES WERE EXPLORED USING ZN(II) AND CU(II) METAL IONS.
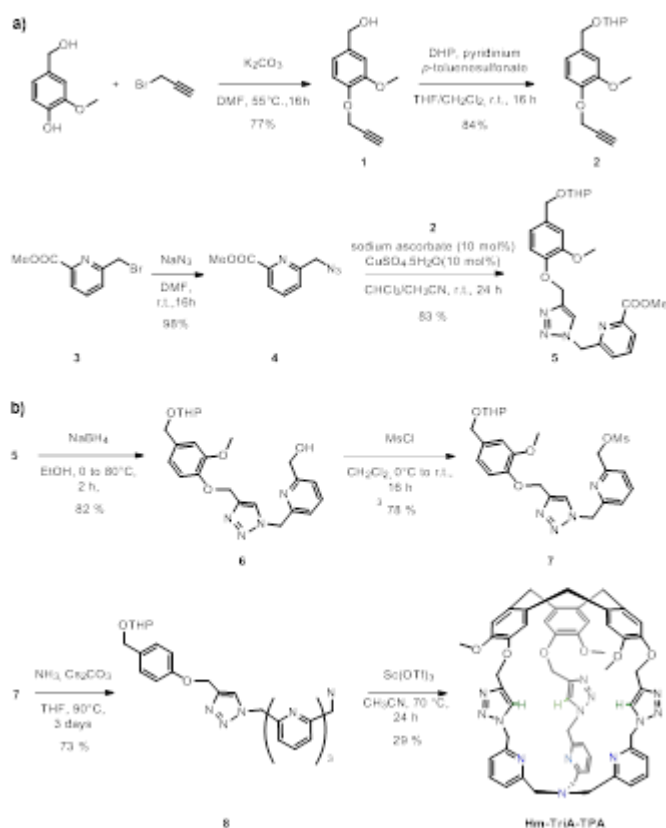
The binding cavities found in metalloproteins govern reaction's selectivity and efficiency. In their hydrophobic channels, destabilizing (like steric repulsion) and stabilizing (like hydrogen bonding, H-bonding) forces, allow for specific enzyme-substrate interactions, substrate positioning and activation/stabilization of highly reactive intermediates.[1] H-bonding is particularly important in metalloenzymes involved in dioxygen processing, such as copper-containing oxygenases and oxidases. The postulated oxidative active species of these systems is the highly reactive mononuclear cupric superoxide (Cu^{II}-O$_2$•⁻).[2] Many efforts have been dedicated to the development of artificial Cu ligands able to generate and stabilize such metastable intermediate. Among them, the tris(2-pyridylmethyl)amine (**TPA**) ligand has been widely used as scaffold for mimicking the first coordination sphere in structural and functional models of copper,[3] but also iron,[4] mono-oxygenases. Interestingly, incorporating intramolecular H-bonding secondary spheres to the **TPA** ligand, was reported as an efficient strategy to stabilize either mononuclear hydroperoxo [(L)Cu^{II}-OOH]$^+$,[5] binuclear peroxodicopper [{(L)Cu^{II}}$_2$(O$_2$$^{2-}$)],[6] or end-on superoxo [(L)Cu^{II}-O$_2$•⁻][7] copper-dioxygen intermediates.

On another side, synthetic supramolecular chemistry is a powerful tool to build cage-like second coordination sphere around bioinspired catalysts.[8] In particular, the archetypal **TPA** ligand has been equipped with well-defined cavities by mean of its covalent substitution,[9, 10] or host-guest encapsulation into an H-bonded capsule.[11] In this context, **TPA**-based hemicryptophanes are organic cages built from a bowl-shaped cyclotriveratrylene (CTV) cap, connected to the tripodal ligand via three linkers. We have recently demonstrated that **TPA**- hemicryptophanes displaying methylene or phenyl linkers, could respectively control the helical arrangement of the ligand,[12] and lead to enhanced oxidation catalysts. [13] However, the hydrophobic cavities found in such cages were devoid of H-bonding groups that could allow substrate positioning or intermediate stabilization.

Despite these progresses, the preparation of **TPA**-based complexes combining hydrophobic cavities with intramolecular H-bonding units at their secondary sphere is still needed. Designing and discovering new methodologies to prepare such advanced model complexes is in fact crucial to better reproduce the key structural properties of metalloenzymes. Beside their connecting benefits, triazole bridges are particularly interesting due to their H-bonding donor properties. For instance, a triazolo organic cage has been recently reported as the most efficient chloride-binding receptor to date, by mean of C$_{triazole}$-H H-bonding interactions.[14] We therefore envisioned that the covalent substitution of the **TPA** by another *C$_3$* symmetrical cap, using triazole spacers, will represent an efficient strategy to construct functionalized cavities.

In this communication, we report the preparation of unprecedented bioinspired complexes displaying a hydrophobic cavity offering three H-bonding triazoles, aiming at reproducing the metalloenzyme's functionalized hydrophobic channels. We design the hemicryptophane **Hm-TriA-TPA** where the archetypal **TPA** ligand is linked to a northern CTV cap, via three triazole bridges, resulting in an H-bond donor decorated cavity.

Hm-TriA-TPA was prepared in an eight-step synthetic strategy (Scheme 1). The cage's walls were first prepared (Scheme 1a), before generating the southern **TPA** and the CTV cap in a final intramolecular macrocyclization closing the structure (Scheme 1b). The aryl propargyl ether derivative **2** was prepared in twosteps by alkylation of the starting vanillyl alcohol with propargyl bromide, followed by the protection of the resulting alcohol **1** with THP. **2** was then connected to the pyridine derivative **4** by a triazole link formed in a Cu-catalyzed azide-alkyne cycloaddition reaction (CuAAC). The CuAAC reaction between equimolar amounts of the propargyl **2,** and the azide **4** precursors, catalyzed by CuSO$_4$ (10 mol%) in the presence of the sodium ascorbate reducing agent (10 mol%), resulted in the formation of the triazole **5** in 83% yield. Precursor **7** was then prepared in two steps by reduction of **5** into the alcohol **6** followed by it mesylation. The addition of ammonia to **7** in the presence of Cs$_2$CO$_3$, at 90°C in THF, afforded the open **TPA** derivative **8** in 73% yield. Formation of **Hm-TriA-TPA** was finally achieved in a 29% yield, via the intramolecular cyclization of **8** in CH$_3$CN, catalyzed by the Lewis acid scandium triflate [Sc(OTf$_3$)], under diluted conditions.

Scheme 1. (a) Synthesis of the pyridine-triazole precursor **5**. (b) synthesis of the targeted hemicryptophane **Hm-TriA-TPA**.

The ^{1}H NMR spectrum of **Hm-TriA-TPA** indicates a C_3 symmetrical structure on average, in CDCl$_3$, at 298K (Fig. 1a). Identical, sharp and well-defined signals could be observed for the protons belonging to the northern CTV unit (H$_h$, H$_i$, H$_j$ and H$_{k,k'}$), the -CH$_2$- links (H$_{e,e'}$ and H$_{g,g'}$), the C$_{triazole}$-H bonds (H$_f$) and the southern **TPA** (H$_{a,a'}$, H$_b$, H$_c$ and H$_d$). 2D-NMR experiments (see the ESI) were used to assign these resonances. Slow diffusion of Et$_2$O to a CH$_2$Cl$_2$ solution of **Hm-TriA-TPA** afforded single crystals suitable for X-ray diffraction. The XRD structure of **Hm-TriA-TPA** confirms the endohedral functionalization of the **TPA** unit by the bowl-shaped CTV via the three triazole bridges having their C$_{triazole}$-H bonds pointing toward the inside of the cavity (Fig. 1b). It should be noted that, in the X-ray structure of the cage, a pyridine unit of the **TPA** reside inside the cavity. This C_1 symmetrical conformation observed in the solid state, contrasts with the symmetrical ^{1}H NMR spectrum of **Hm-TriA-TPA** in solution. Fast conformational exchanges between in-out orientation of the pyridines could explain this behavior in solution at 298K.
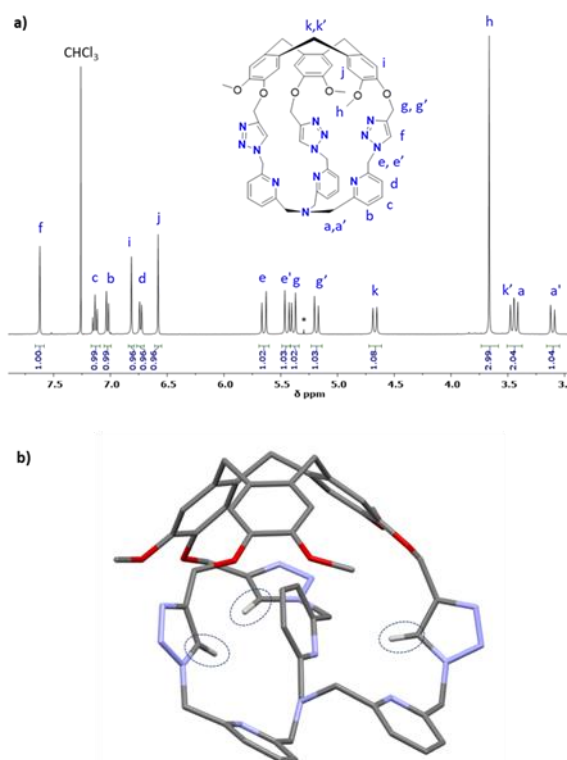
Figure 1. (a) ^{1}H NMR spectra (CDCl₃, 400 MHz) of **Hm-TriA-TPA** along with (b) view of its X-ray crystal structure. Only the hydrogen atom belonging to the three triazole units have been included for clarity.

We have then investigated the ability of our caged ligand to form metallo-complexes in solution via coordination at its **TPA** unit. Binding of the air-stable and diamagnetic zinc triflate salt $Zn^{II}(OTf)_2$, was monitored by ^{1}H-NMR in CD₃CN at 298K (Fig. 2 and Fig. S6 ,ESI). The ^{1}H-NMR spectra of **Hm-TriA-TPA** in the presence of 0.5 equiv. of the zinc salt reveal two sets of signals for each protons of the cage, that could be attributed to the presence of **Zn^{II}(Hm-TriA-TPA)(OTf)₂** and **Hm-TriA-TPA** in a 1:1 ratio (Fig. 2b). Interestingly, in the presence of a stoichiometric amount of the metal salt, the resonances belonging to the free cage fully disappear to the profit of the zinc complex signals, indicating full complexation. Upon metalation, a strong down-field shift occurs on the protons of the **TPA**'s pyridines (H_b, H_c and H_d, $\square_{ppm}$: 0,35- 0,7 ppm) that remain equivalent. The triazole bridges appear less affected with a modest upfield-shift observed for the $C_{triazole}$-H bond (H_f, $\square_{ppm}$<0,03 ppm). Overall, the ^{1}H-NMR analysis of **Zn^{II}(Hm-TriA-TPA)(OTf)₂** attests for retained C_3 symmetry of the caged ligand (on average) with identical and sharp signals for every resonances. Altogether, these observations unambiguously confirm the coordination of the Zn^{II} metal ion at the **TPA** unit with retention of the endohedral functionalization of the resulting complex.[12] This was further supported by the optimized DFT (Density Functional Theory) structure that clearly reveals a C_3 symmetrical caged Zn(II) complex in a trigonal bipyramidal geometry with an apical molecule of acetonitrile (Fig. 2e, Fig. S7, ESI). Finally, identical spectra were observed upon addition of a second equivalent of **Zn^{II}(OTf)₂** (Fig. 2d), ruling out the possibility of a second metal-binding event occurring at the triazole crown.[15]
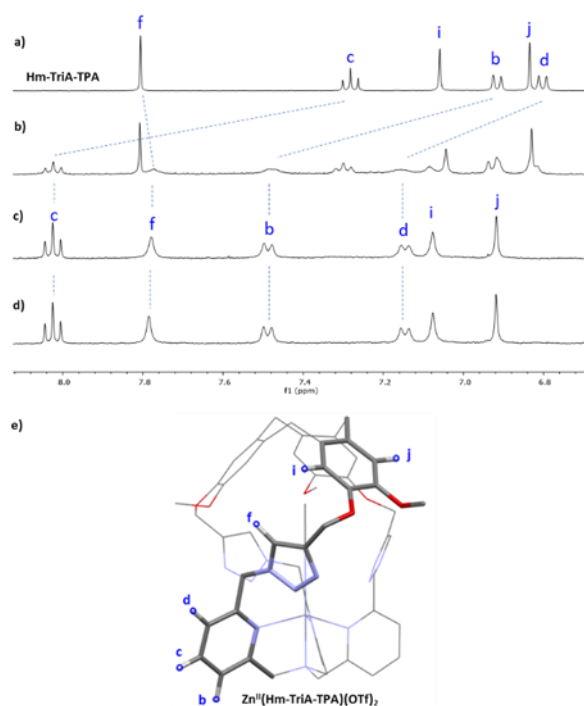
Figure 2. Monitoring of the ^{1}H NMR spectra (CD$_3$CN, 400 MHz) of **Hm-TriA-TPA** (a), upon addition of 0.5 equiv. (b), 1.0 equiv. (c) and 2.0 equiv. (d) of Zn(OTf)$_2$ (depicted region: 6.7 – 8.1 ppm). (e) DFT-optimized structure (PBE0-D3/def2-TZVP, COSMO, see ESI for full computational details) of **Zn^{II}(Hm-TriA-TPA)(OTf)$_2$**.

We have next investigated the possibility of preparing Cu^{II} complexes at our caged ligand. The **Cu^{II}(Hm-TriA-TPA)(OTf)$_2$** complex was prepared by reacting the ligand with stoichiometric amounts of Cu^{II}(OTf)$_2$ in CH$_3$CN, at room temperature (see ESI). Formation of the targeted complex, in a 1:1 stoichiometry, was evidenced by High-Resolution Mass Spectrometry analysis (ESI-HRMS, Fig. S8, ESI). Furthermore, crystallization by slow diffusion of diethyl ether to a CH$_3$CN solution of the complex affords single crystals suitable for X-ray diffraction, allowing for determination of its solid-state structure. The structure of the **Cu^{II}(Hm-TriA-TPA)(OTf)$_2$** complex shows a pentacoordinated copper center in a distorted square pyramidal geometry (Fig. 3a). The distorted tetragonal plane comprises the tertiary amine (N1), two pyridines (N2 and N3), and one triazole (N5) in *trans* to the tertiary amine with similar Cu-N bond length ranging from 1.978 Å to 2.055 Å. The coordination sphere is completed by an apical pyridine (N4) with a Cu-N distance of 2.225 Å. Importantly, a well-defined cavity, described by the northern CTV unit and the tris-triazole crown could be observed just above the Cu^{II} center confirming its endohedral functionalization. The latter is occupied by a non-bonded guest molecule of acetonitrile (solvent).

Could the Cu-triazole bond in **Cu^{II}(Hm-TriA-TPA)(OTf)$_2$** be replaced by anion coordination at the Cu^{II}-**TPA** core ?

Anion binding at Cu-**TPA** derivatives has been reported to result in trigonal-bipyramidal Cu(II) complexes with axial binding of the anion in *trans* to the tertiary amine.[16] Among them, azido adducts [(Cu^{II}-**TPA^X**)(N$_3^-$)]$^+$ have been described as electronic and structural analogues of cupric superoxide intermediates [(Cu^{II}-**TPA^X**)(O$_2$$^{\bullet-}$)]$^+$. The N$_3^-$ anion binds to Cu^{II}-**TPA** complexes with very similar bond lengths and angles (Cu^{II}-N-N) to those found in [(Cu^{II}-**TPA^X**)(O$_2$$^{\bullet-}$)]$^+$.[7] Azido complexes(Cu^{II}-**TPA^X**)(N$_3^-$)]$^+$ have been extensively studied by electronic and vibrational spectroscopies.[11] They display typical azido → Cu^{II} LMCT transitions, and ν(N-N) stretching frequency. On this basis, we explored the possibility of binding N$_3^-$ to our caged Cu(II) complex. UV-vis analysis of **Cu^{II}(Hm-TriA-TPA)(OTf)$_2$**, in acetone, reveal typical d-d transition centered at 634 nm (0,5 mM, ε = 139 M^{-1} cm^{-1}, Fig. S9, ESI). The UV-vis monitored addition of tetrabutylammonium azide NBu$_4$N$_3$ to a 0,5 mM solution of the caged complex, in acetone, results in the appearance of an intense absorption band centered at 415 nm (LMCT, ε = 2068 M^{-1}cm^{-1}) and a d-d band at 713 nm (ε = 249 M^{-1} cm^{-1}, Fig. 3b). The final spectrum was identical to that of the azido adduct prepared using NaN$_3$ and isolated by precipitation (see ESI).
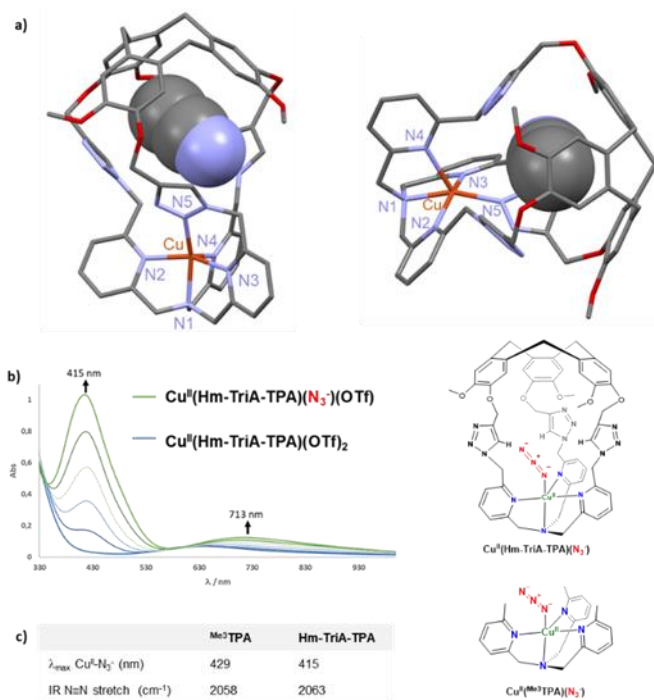
Figure 3. (a) Views of the X-ray crystal structure of **Cu^{II}(Hm-TriA-TPA)(OTf)$_2$** (b) UV-vis monitoring of the formation of the azido adduct **Cu^{II}(Hm-TriA-TPA)(N$_3$)(OTf)**, upon addition of NBu$_4$N$_3$ (0 to 1.0 equiv.) to a 0,5 mM solution of **Cu^{II}(Hm-TriA-TPA)(OTf)** in acetone. (c) spectroscopic features (UV-vis and IR) of the azido complexes stabilized by **^{Me3}TPA** and **Hm-TriA-TPA**.

These UV-vis data are consistent with the formation of the azido complex **Cu^{II}(Hm-TriA-TPA)(OTf)(N$_3$)**.[2, 7, 11] In **TPA**-complexes bearing intramolecular H-bonding donors, the potential presence of stabilizing interactions with the azido moiety has been associated to a blue-shift of the LMCT band, as well as a blue-shift of the $\square$(N-N) stretching frequency.[2,17] Value of the LMCT band observed in the case of **Hm-TriA-TPA** was therefore compared with the one of its corresponding open model ligand **^{Me3}TPA** devoid of intramolecular H-bonding groups (Fig 3c). Compared to the open **TPA**-based complex **Cu^{II}(^{Me3}TPA)(OTf)(N$_3$)** ($\square_{max}$ = 429nm, Fig. S10, ESI), the Cu^{II}-N$_3^-$ LMCT bands in our triazole-containing cage shift to higher energy ($\square_{max}$ = 415nm). Finally, to further support the stabilization offer by **Hm-TriA-TPA**, the two azido complexes have been isolated and they antisymmetric N$_3^-$ IR stretch compared. Interestingly, **Cu^{II}(Hm-TriA-TPA)(OTf)(N$_3$)** displays a 5 cm^{-1} blue-shift of the $\square$(N-N) stretching frequency compared to the "base" ligand **^{Me3}TPA** (Fig. 3c, Fig. S11 and S12, ESI). These findings are therefore consistent with a bonding stabilization of the azido adduct within the triazole-containing cavity.

Conclusions

In summary, the preparation of an organic cage where the canonical **TPA** ligand is surmounted by a H-bonding hydrophobic cavity offering three triazole units is described. We demonstrate that this cage can coordinate zinc(II) and copper(II) metal ions at its **TPA** unit with an endo-functionalization of the complex, in both solution and solid state. These are the first examples of bioinspired complexes equipped with a tris-triazole decorated cavity mimicking the functionalized (H-bonding) hydrophobic channels of metalloenzymes. Finally, we found that the azidocopper(II) adduct [(L)Cu^{II}-N$_3^-$] can be prepared upon addition of N$_3$ to the caged Cu(II) complex. Spectroscopic analysis of this structural analogue of the cupric superoxide intermediates [(L)Cu^{II}-O$_2^{\bullet-}$], suggest stabilization of the azido adduct, within the C$_{triazole}$-H based cavity. We envision that our strategy might finds applications toward the development of non-enzymatic catalysts able to stabilize reactive intermediates and/or control substrate positioning by their H-bonding hydrophobic cavity. Future work will focus on the use of **TPA** ligands equipped with our triazole-functionalized cavity to generate, stabilize, and explore the reactivity of end-on superoxocopper(II) complexes upon dioxygen activation.

Notes and references[18]

[1]   Z. Wojdyla and T. Borowski, *Chem. Eur. J.*, 2022, DOI: 10.1002/chem.202104106

[22]   M. A. Ehudin, A. W. Schaefer, S. M. Adam, D. A. Quist, D. E. Diaz, J. A. Tang, E. I. Solomon and K. D. Karlin, *Chem. Sci.*, 2019, **10**, 2893-2905

[3]   S. Y. Quek, S. Debnath, S. Laxmi, M. van Gastel, T. Krämer and J. England, *J. Am. Chem. Soc.* 2021, **143**, 19731–19747

[4]   M. Borrell, E. Andris, R. Navrátil, J. Roithová and M. Costas, *Nat. Commun.*, 2019, **10**, 901

[5]   A. Wada, M. Harata, K. Hasegawa, K. Jitsukawa, H. Masuda, M. Mukai, T. Kitagawa, and Hisahiko Einaga, *Angew. Chem. Int. Ed.* 1998, **37**, 798-799

[6]   E. W. Dahl, H. T. Dong and N. K. Szymczak, *Chem. Commun.*, 2018, **54**, 892-895

[7]   (a) M. Bhadra, J. Yoon C. Lee, R. E. Cowley, S. Kim, M. A. Siegler, E. I. Solomon, and K. D. Karlin, *J. Am. Chem. Soc.* 2018, **140**, 9042−9045, (b) D. E. Diaz, D. A. Quist, A. E. Herzog, A. W. Schaefer, I. Kipouros, M. Bhadra, E. I. Solomon, and K. D. Karlin, *Angew. Chem. Int. Ed.* 2019, **58**, 17572–17576

[8]   (a) S. C. Bete, and M. Otte*, Angew. Chem. Int. Ed.* 2021, **60**, 18582 –18586, (b) C. Colomban, V. Martin-Diaconescu, T. Parella, S. Goeb, C. García-Simón, J. Lloret-Fillol, M. Costas, and X. Ribas, *Inorg. Chem.*, 2018, **57**, 3529–3539

[9]   C. Bravin, E. Badetti, G. Licini, C. Zonta, *Coordination Chemistry Reviews*, 2021, **427**, 213558

[10]   N. Le Poul, B. Colasson, G. Thiabaud, D. Jeanne Dit Fouque, C. Iacobucci, A. Memboeuf, B. Douziech, J. Řezáč, T.Prangé, A. de la Lande, O. Reinaud and Y. Le Mest, *Chem. Sci.*, 2018, **9**, 8282-8290

[11]   T. Zhang, L. Le Corre, O. Reinaud, and B. Colasson, *Chem. Eur. J.* 2021, **27**, 434-443

[12]   G. Qiu, C. Colomban, N. Vanthuyne, M. Giorgi and A. Martinez, *Chem. Commun.*, 2019, **55**, 14158–14161.

[13]   S. A. Ikbal, C. Colomban, D. Zhang, M. Delecluse, T. Brotin, V.Dufaud, J. P. Dutasta, A. B. Sorokin and A. Martinez, *Inorg. Chem.*, 2019, **58**, 7220-7228

[14]   Yun Liu, Wei Zhao, Chun-Hsing Chen and Amar H. Flood, *Science*, 2019, **365**, 159-161

[15]   Identical ^{1}H-NMR spectra was obtain after isolation of the Zn complex by precipitation with Et_2O (Fig. S6, ESI)

[16]   C. M. Moore and N. K. Szymczak, *Chem. Commun.*, 2015, **51**, 5490-5492

[17]   A. Wada, Y. Honda, S. Yamaguchi, S. Nagatomo, T. Kitagawa, K. Jitsukawa, and H. Masuda, *Inorg. Chem.* 2004, **43**, 5725-5735